

# Atomic and electronic structure of the Si(001)2×2-Li chemisorption system at 0.5 monolayer coverage

H. Q. Shi, M. W. Radny, and P. V. Smith

*School of Mathematical and Physical Sciences, The University of Newcastle, Callaghan, Australia, 2308*

(Received 5 August 2003; revised manuscript received 14 January 2004; published 30 June 2004)

*Ab initio* plane-wave pseudopotential density functional theory (DFT) calculations have been carried out to determine the atomic and electronic structure of the Si(001)2×2-Li adsorption system at 0.5 monolayer (ML) coverage. The minimum energy configuration is found to be characterized by alternating symmetric and asymmetric Si-Si dimers along each dimer row independently of the details of the Li adatom topology. This is due to virtually all of the Li charge being transferred to just one of the dimers in each 2×2 surface unit cell, leaving the second dimer essentially unchanged. The nature and dispersion of the theoretically predicted occupied electronic surface state bands are found to be in good agreement with the angle-resolved photoemission data and little dependent on the actual Li adatom geometry. The composition of the second and third lowest unoccupied surface state bands, however, clearly depends on the Li adatom topology. The nature of the lowest energy unoccupied surface state band suggests that the Si(001)-Li chemisorption system at 0.5 ML coverage will exhibit a reactivity similar to that of the clean Si(001) surface.

DOI: 10.1103/PhysRevB.69.235328

PACS number(s): 68.35.Bs, 68.43.-h, 73.20.-r

## I. INTRODUCTION

The chemisorption of alkali metals (AM) on the Si(001) surface has been an important area of research for almost three decades.<sup>1-3</sup> Most of this work has been focused on understanding the interaction of sodium, potassium, and cesium with the (001) surface of silicon, and comparatively little effort has been devoted to studying the Si(001)-Li chemisorption system.<sup>4-17</sup> *Ab initio* plane-wave pseudopotential density functional theory (DFT) calculations of the Si(001)2×1-Li adsorption system at 1.0 monolayer (ML) coverage<sup>18,19</sup> have shown that charge transfer from the Li adatoms to the Si dimer atoms leads to a transition from the asymmetric dimers of the clean Si(001) surface, to symmetric dimers for the Li chemisorbed surface at monolayer coverage, in agreement with the experimental results of Johansson *et al.*<sup>9</sup> and Grehk *et al.*<sup>10</sup> The predicted electronic structure<sup>18</sup> was also found to be in good agreement with the photoemission data of Kim *et al.*<sup>13</sup> and Johansson and Reihl.<sup>5</sup> The aim of this paper is to perform similar calculations for the Si(001)-Li chemisorption system at 0.5 ML coverage.

Kim *et al.*<sup>8</sup> used low energy electron diffraction (LEED) to study the lithium induced reconstructions of the Si(001) surface at room temperature or below, and found that increasing the Li coverage produced a series of ordered phases: (2×2):Li→(2×1):Li→ $c(3\sqrt{2}\times\sqrt{2})R45^\circ$ :Li→streaky  $c(3\sqrt{2}\times\sqrt{2})R45^\circ$ :Li→(4×1):Li→(1×1):Li. To explain these results, these authors proposed a structural model in which the adsorbed Li adatoms flip (reverse) the buckling of the asymmetric Si-Si surface dimers. This led to the proposal that the (2×2):Li phase corresponds to the buckled Si-Si dimers having a ferromagnetic and antiferromagnetic arrangement along the  $[1\bar{1}0]$  and  $[110]$  directions, respectively (see Fig. 1). The idea that the Si(001)-Li chemisorption system at 0.5 ML coverage is characterized by buckled dimers is consistent with the results obtained from the high resolu-

tion core-level spectroscopy studies of Johansson *et al.*<sup>9</sup> and Grehk *et al.*<sup>10</sup> These measurements indicated that below 1.0 ML coverage, the basic dimer structure of the clean Si(001) surface was preserved (i.e., the dimers were asym-

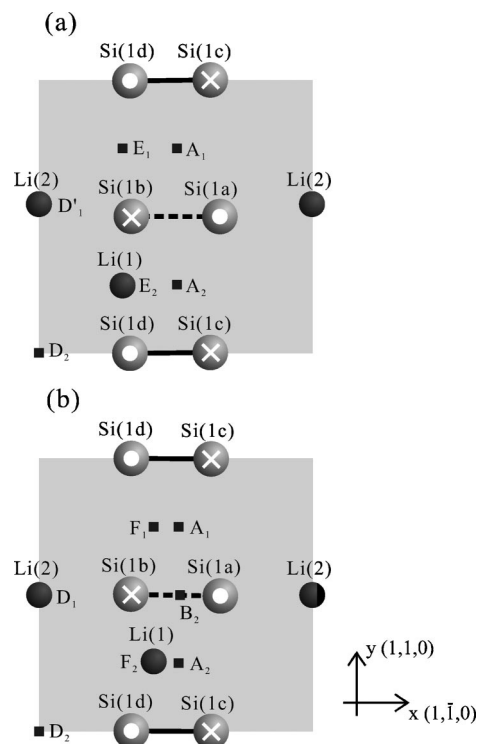


FIG. 1. Top views of the two essentially degenerate minimum energy configurations for the Si(001)2×2-Li chemisorption system at 0.5 ML coverage. The various possible chemisorption sites are denoted by the symbols A–F. The gray area denotes the 2×2 SUC. The dashed line indicates the weakly buckled dimer and a solid line represents a strongly buckled dimer. The ● and × signs indicate up and down atoms, respectively.

metric). There is, however, no direct data on the actual chemisorption sites occupied by the Li adatoms on the Si(001) surface for coverages below 1.0 ML. In the early studies of AM-Si(001) chemisorption systems it was assumed that Levine's model<sup>20</sup> for Cs adsorption on the Si(001) surface would be valid for all of the AM's at 0.5 ML coverage. In this model, the AM atoms are positioned above each Si(001) $2 \times 1$  dimer row at the pedestal sites between neighbouring Si-Si dimers (these sites are labeled A in Fig. 1). Morikawa *et al.*<sup>17</sup> studied the Si(001) $2 \times 1$ -Li system at 0.5 ML coverage using a first-principles molecular dynamics method. These calculations predicted that the Li adatoms would sit directly above the second layer Si atoms, rather than the third layer sites as assumed in the Levine model. Similar results were obtained by Ko *et al.*<sup>19</sup> from calculations employing a Si(001) $2 \times 2$  surface unit cell (SUC). In contrast to Morikawa *et al.*,<sup>17</sup> however, they predicted that one of the two Si dimers within each  $2 \times 2$  SUC relaxed to a nearly symmetric structure, while the second one retained its buckled topology.

The surface electronic structure of the Si(001) $2 \times 2$ -Li system was studied experimentally by Kim *et al.*<sup>13</sup> using angle resolved ultraviolet photoelectron spectroscopy (ARUPS), and was found to be noticeably different from that of the clean Si(001) surface. It also displayed some features that were different to those exhibited by the other alkali metals. This latter observation is consistent with the ARUPS and IPES measurements of Johansson and Reihl<sup>5</sup> which showed that Li adsorption on Si(001) is quite different to that of Na and K. The photoemission experiments by Johansson and Reihl also revealed an AM-induced unoccupied surface state that shifted downwards in energy with increasing coverage. Johansson and Reihl<sup>5</sup> also found that the highest occupied surface state band split into two peaks with increasing AM adsorption. The electronic structure of the Si(001) $2 \times 2$ -Li chemisorption system at 0.5 ML coverage has been calculated by Ko *et al.*<sup>19</sup> No attempt, however, has been made to compare the results of theoretical studies of this system with the experimental data.

The main objective of this paper is to report the results of accurate first-principles calculations of the atomic and electronic structure of the Si(001) $2 \times 2$ -Li system at 0.5 ML coverage, and to compare these results with the currently available experimental data, and other theoretical calculations. Two essentially isoenergetic structures have been determined to be the most stable. These structures were found to be topologically different, and  $\sim 0.17$  eV per  $2 \times 2$  SUC more stable, than the minimum energy configuration found by Ko *et al.*<sup>19</sup> The Si surface dimers associated with our minimum energy Li-chemisorbed structures, on the other hand, were very similar to those found by Ko *et al.* with one dimer having a large buckling angle, and the other being relatively flat. The calculated electronic structure is shown to be in good agreement with the photoemission data.

## II. METHOD AND PROCEDURE

All of the calculations have been performed using the *ab initio* total energy and molecular dynamics program VASP

TABLE I. The energies (in eV) of the different atomic configurations of the Si(001) $2 \times 2$ -Li chemisorption system for 0.5 ML coverage, relative to that of the lowest energy configurations. The notation for the various sites is the same as that in Fig. 1.

Configuration	Energy
$E_2-D'_1, F_2-D_1$	0.00
$E_1-E_2$	0.17
$E_2-A_1$	0.19
$F_1-F_2$	0.23
$B_2-D_1$	0.27
$D_2-D_1$	0.48

(Vienna *ab initio* simulation package),<sup>21-23</sup> which is based on the density functional pseudopotential plane wave method. For our  $2 \times 2$  periodic unit cell we have employed 6 silicon layers plus 8 hydrogen atoms to saturate the dangling bonds of the bottom layer silicon atoms, together with a vacuum region of  $\sim 8$  Å. The minimum energy structures were found by allowing all of the coordinates of the silicon atoms in the top four layers of the slab, plus those of the chemisorbed lithium atoms, to vary. PAW potentials<sup>24</sup> were used to describe the lithium, silicon and hydrogen atoms. The Kohn-Sham equations were solved using 4 special  $\mathbf{k}$  points in the irreducible symmetry element of the Si(001) $2 \times 2$  SBZ, and employing plane waves with kinetic energies of up to  $\sim 20$  Rydbergs. To identify the electronic surface states we have calculated the function  $\rho_{n\mathbf{k}}(z)$  defined by

$$\rho_{n\mathbf{k}}(z) = \int_{\text{SUC}} |\Psi_{n\mathbf{k}}(x, y, z)|^2 dx dy,$$

where  $x$  and  $y$  lie in the surface plane,  $z$  is out of the surface, and the integration is performed over the SUC. Three-dimensional (3D) charge/probability density distributions were also calculated to help delineate the nature of the individual surface state bands. States were identified as surface states (or resonances) if the  $\rho_{n\mathbf{k}}(z)$  function showed clear exponential decay into the bulk and the corresponding density plots evidenced large surface contributions with smaller contributions from the bulk layers.

## III. RESULTS

### A. Atomic structure

To reliably determine the minimum energy structure for the Si(001) $2 \times 2$ -Li chemisorption system at 0.5 ML coverage we performed geometry optimization calculations using many different configurations for the two lithium atoms in each  $2 \times 2$  SUC. Energy values for the most stable of these structures are presented in Table I. Two structures with virtually identical energy were found to be the most stable. The first of these structures, the  $E_2-D'_1$  configuration, is shown in Fig. 1(a). In this structure, the Li(1) atom sits to the left of the midpoint between the silicon atoms at the end of two adjacent dimers of the same dimer row (at the  $E_2$  site), while the Li(2) atom is positioned a small distance along the posi-

TABLE II. Optimized geometry (in Å) of the Si(001)2×2-Li chemisorption system at 0.5 ML coverage for our two essentially degenerate minimum energy structures.  $\Delta z$  is the vertical displacement relative to the ideal bulk terminated surface, and  $d$  denotes the various bond lengths in Å.

	Figure 1(a)	Figure 1(b)
$\Delta z_{\text{Li}(1)}$	1.59	1.50
$\Delta z_{\text{Li}(2)}$	0.38	0.65
$\Delta z_{\text{Si}(1a)}$	0.17	0.17
$\Delta z_{\text{Si}(1b)}$	0.04	0.03
$\Delta z_{\text{Si}(1c)}$	-0.65	-0.68
$\Delta z_{\text{Si}(1d)}$	-0.05	-0.05
$d_{\text{Si}(1a)-\text{Si}(1b)}$	2.47	2.50
$d_{\text{Si}(1c)-\text{Si}(1d)}$	2.32	2.31
$d_{\text{Li}(1)-\text{Si}(1b)}$	2.49	2.47
$d_{\text{Li}(1)-\text{Si}(1d)}$	2.51	2.56
$d_{\text{Li}(2)-\text{Si}(1a)}$	2.62	2.63
$d_{\text{Li}(2)-\text{Si}(1b)}$	2.62	2.63

tive  $y$  axis from the long-bridge (cave) site (at the  $D'_1$  site). In the second structure, the  $F_2$ - $D_1$  configuration, shown in Fig. 1(b), the Li(1) atom moves to the right of the midpoint towards the pedestal site to occupy the  $F_2$  site, while the Li(2) atom sits essentially at the cave site  $D_1$ . In both cases, the Li(1) atom is displaced some distance along the negative  $x$  direction from the A site proposed by Levine,<sup>20</sup> while the Li(2) atom occupies a quite different position within the  $2 \times 2$  SUC.

Three of the seven structures listed in Table I were also investigated by Ko *et al.*<sup>19</sup> These are the  $E_1$ - $E_2$ ,  $B_2$ - $D_1$ , and  $D_2$ - $D_1$  configurations. In the paper by Ko *et al.*<sup>19</sup> these are referred to as the  $B_2$ - $B_2$ , HB- $T_4$ , and  $T_4$ - $T_4$  configurations, respectively. The  $E_1$ - $E_2$  structure in which both Li atoms occupy E sites is the minimum energy structure determined by Morikawa *et al.*<sup>17</sup> and Ko *et al.*<sup>19</sup> employing a  $2 \times 1$  SUC and  $2 \times 2$  SUC, respectively. Ko *et al.* found the  $B_2$ - $D_1$  and  $D_2$ - $D_1$  structures to be 0.05 eV and 0.16 eV per lithium atom less stable, respectively, than that of the  $E_1$ - $E_2$  structure. Our calculations yield the values 0.051 eV and 0.153 eV. It follows that our results are in excellent agreement with those of Ko *et al.* Our results differ, however, in that we have determined two additional configurations ( $E_2$ - $D'_1$  and  $F_2$ - $D_1$ ) which are substantially lower in energy (by  $\sim 0.17$  eV) than the  $E_1$ - $E_2$  configuration predicted by Morikawa *et al.*<sup>17</sup> and Ko *et al.*<sup>19</sup> Both of our minimum energy structures are also quite different topologically from the models proposed by Levine,<sup>20</sup> Morikawa *et al.*,<sup>17</sup> and Ko *et al.*<sup>19</sup> in which the two lithium atoms occupy topologically equivalent sites.

The atomic relaxations, and various bond lengths of interest, for our two lowest energy structures, are presented in Table II. In order to analyze the reconstruction of the substrate induced by the chemisorption of the Li atoms, we have also optimized the geometry for the Si(001)2×2 clean surface using PAW potentials. We found two alternately buckled dimers with buckling angles of 19.4° and bond lengths of

2.34 Å. These results are in good agreement with the plane wave pseudopotential calculations of Ramstad *et al.*<sup>25</sup> which predicted that the optimized dimer structure for the Si(001)2×2 clean surface is alternately buckled with buckling angles of around 19.1° and bond lengths of 2.28 Å. Comparing our minimum energy lithium adsorption topology in Fig. 1(a) and 1(b) with that of the clean Si(001)2×2 surface, we find that one of the buckled dimers of the Li-chemisorbed Si(001)2×2 surface retains its original nature with a relatively large buckling angle of -14.5° (-15.2°) and dimer bond length of 2.32 (2.31) Å, while the other oppositely buckled dimer significantly changes its character. The bond length of 2.47 (2.50) Å of this latter dimer is significantly longer than that of the clean Si(001)2×2 surface, and its buckling angle of 3.2° (3.2°) much smaller. It is thus clear that lithium adsorption on the Si(001)2×2 surface at 0.5 ML coverage significantly changes one of the dimers of the Si(001)2×2 clean surface, while keeping the other dimer almost the same. Interestingly, an almost identical geometry for the reconstructed Si(001)2×2 substrate was predicted by Ko *et al.*<sup>19</sup> for their topologically different  $E_1$ - $E_2$  0.5 ML Li adatom configuration. These results are consistent with the model proposed by Kim *et al.*<sup>8</sup> for the Si(001)2×2-Li chemisorption system at 0.5 ML coverage in which asymmetric dimers are arranged ferromagnetically perpendicular to the dimer rows, and antiferromagnetically parallel to the dimer rows. These results also suggest that while neither Li atom bonds to a particular Si dimer atom, the combined interaction of the two lithium atoms with the surface results in the formation of two quite different dimers in each  $2 \times 2$  SUC, one of which is strongly buckled as on the clean Si(001) surface, while the other is only weakly buckled.

## B. Electronic structure

To obtain an initial insight into what happens when two Li adatoms per  $2 \times 2$  SUC chemisorb on the Si(001) surface, we have calculated the difference between the total charge density of the Si(001)2×2-Li system at 0.5 ML coverage and that of the clean Si(001) surface with alternately buckled dimers. The obtained charge density difference is plotted in Fig. 2. We observe that the excess charge of the Si(001)2×2-Li system is mainly distributed around the down Si atom of the symmetric (weakly buckled) Si dimer. This indicates that the charge of approximately  $2e$  is transferred from the two Li adatoms to just one of the two Si dimers present within each  $2 \times 2$  SUC. It is this charge transfer that compensates for the charge deficiency on the down Si atom of that particular dimer. This results in a flattening of that dimer and the formation of the Li chemisorbed Si(001)2×2 surface with one strongly buckled, and one weakly buckled, dimer. It should be noted that this mechanism is the same as that discussed by Ko *et al.*<sup>19</sup> for the chemisorption of lithium on the Si(001)2×2 surface at 0.5 ML coverage. In that case, however, the charge is transferred to one of the Si dimers from Li adatoms chemisorbed at topologically identical sites [the interdimer bridge sites (E) between the Si dimers] rather than from two different and



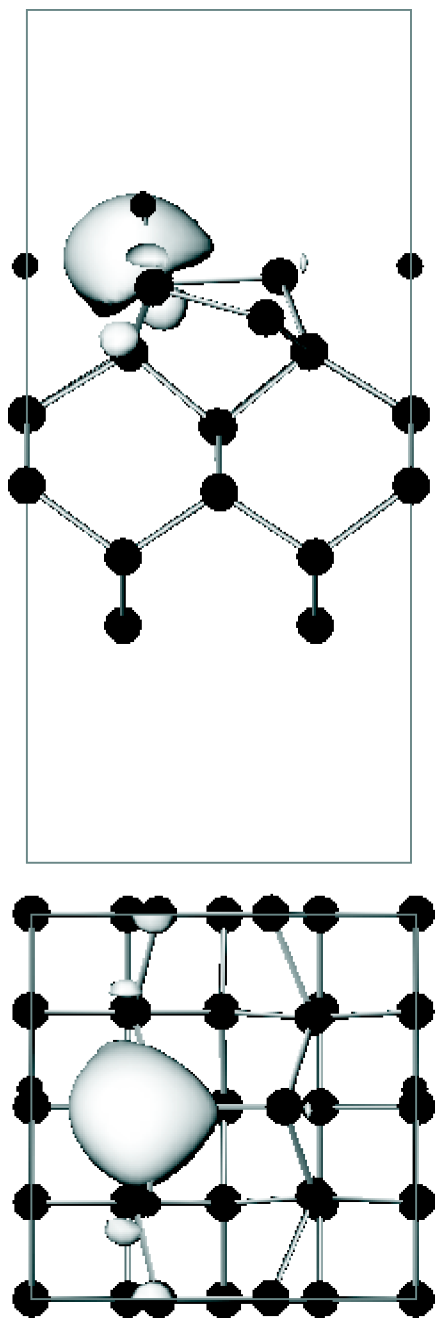


FIG. 2. Side and top views of the 3D charge density difference between the total charge density of the Si(001) $2 \times 2$ -Li surface at 0.5 ML coverage, and the reconstructed Si(001) $2 \times 2$  clean surface with alternately buckled dimers. In this figure, and all subsequent figures, the smaller and larger filled circles denote the lithium and silicon atoms, respectively, and the top view is the same as that in Fig. 1. The plots are for a charge density isosurface value of  $9.1 \times 10^{-2} e/\text{\AA}^3$ .

inequivalent sites. These results show that while the locations of the Li adatoms on the surface are only weakly correlated energetically, the combined interaction of the two lithium atoms with the substrate always results in a highly correlated charge transfer and the formation of one strongly buckled and one weakly buckled Si dimer. The almost identical Si(001) $2 \times 2$  substrate reconstructions induced by topo-

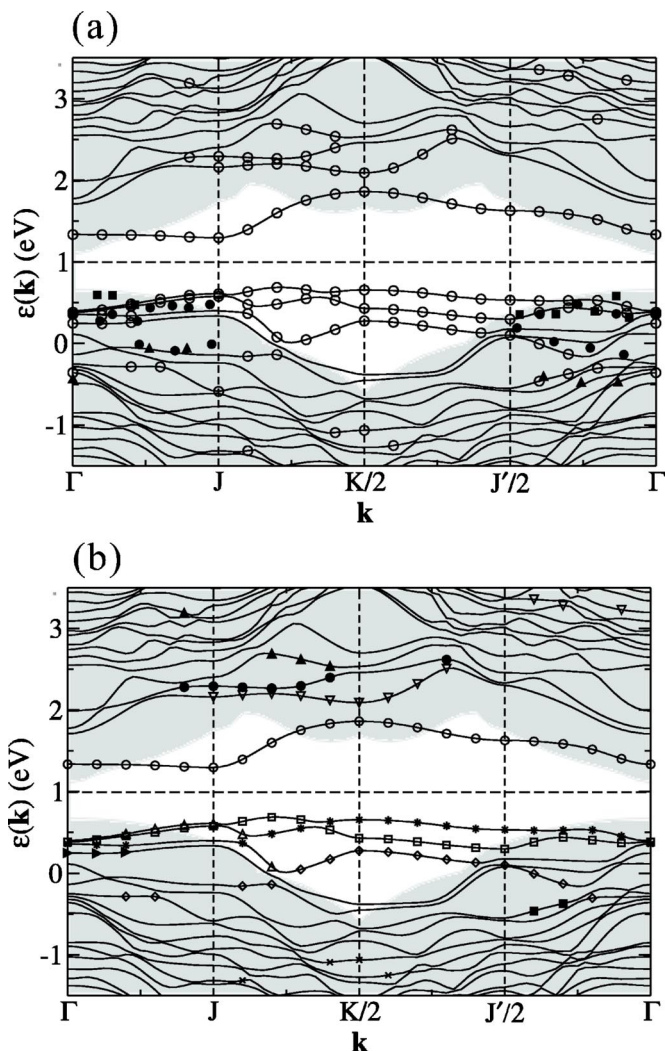


FIG. 3. Surface electronic structure of the Si(001) $2 \times 2$ -Li chemisorption system at 0.5 ML coverage in the vicinity of the Fermi energy. (a) The empty circles indicate the theoretically predicted surface states, and the filled circles and triangles denote the ARUPS data of Kim *et al.* (Ref. 13); (b) Identified surface states: seven occupied (asterisks and crosses, empty diamonds, squares, and triangles, and filled squares and arrow heads), and four unoccupied (empty circles and inverted triangles, and filled circles and triangles). The projected bulk bandstructure is indicated by the gray shaded areas in both figures.

logically different Li adatom configurations also reveals a clear tendency for the Si dimer dangling bond orbitals to be either empty or fully occupied.

In order to see if there were any significant differences between our two theoretically predicted lowest energy structures, we calculated the band structures of both configurations using the VASP program.<sup>21-23</sup> These band structures were found to be virtually identical. We thus expect that a detailed analysis of the electronic structure of these two configurations would also yield very similar behavior. As a result, all of the remainder of this paper will be devoted solely to the structure shown in Fig. 1(a). In Figs. 3(a) and 3(b) we have plotted the energy bands obtained from calculating the eigenvalues in the vicinity of the bulk energy gap at 80 k

points along the  $\Gamma$ -J-K/2-J'/2- $\Gamma$  symmetry directions of the  $2 \times 2$  SBZ. The states that we have identified as surface states from the nature of the associated  $\rho_{nk}(z)$  function and charge/probability density plots, are shown in Fig. 3(a) as the empty circles. The experimental data obtained by Kim *et al.*<sup>13</sup> for the valence-band surface states of the Si(001)2  $\times$  2-Li chemisorption system along the  $\Gamma$ -J and  $\Gamma$ -J'/2 symmetry directions of the SBZ is also shown in Fig. 3(a). The filled circles indicate strong peaks in the angle-resolved photoemission spectra, while the filled squares and triangles denote weak peaks. All of the experimental data has been shifted up by about 0.18 eV to match the theoretically predicted values. This shift is required because of the neglect of self-energy effects in the standard density functional theory.

As can be seen from Fig. 3(a), the agreement between the theoretical results (empty circles) and the experimental data of Kim *et al.* (filled symbols) is very good. While our uppermost occupied surface state band along the  $\Gamma$ -J'/2 symmetry direction of the SBZ does not appear to have been observed in the ARUPS experiments of Kim *et al.*,<sup>13</sup> there is excellent agreement between theory and experiment for the second band which first disperses upward from  $\Gamma$  and then bends downward to J'/2. There is also good correlation between theory and experiment for the other occupied surface states along  $\Gamma$ -J'/2 with both theory and experiment predicting a downward dispersion from J'/2 for the upper band (indicated by the solid circles), and relatively little dispersion for the lower band (solid triangles). Our theoretical results also predict a splitting of the two lowest valence band surface states at the J'/2 symmetry point of 0.197 eV in good agreement with the experimental separation of around 0.16 eV.

Along the  $\Gamma$ -J direction of the SBZ, our calculations reveal the presence of three occupied surface state bands close to the Fermi energy. All three of these bands have very similar energies. The ARUPS experiments of Kim *et al.*<sup>13</sup> also evidenced surface states in this region with similar dispersion [filled circles in Fig. 3(a)]. A weak, fairly flat, lower lying occupied surface state band along the  $\Gamma$ -J direction of the SBZ [indicated by the filled triangles and circles in Fig. 3(a)] was also indicated by the ARUPS data. While our theoretical calculations determine a band in this energy region, the corresponding  $\rho_{nk}(z)$  failed to show any significant localization in the vicinity of the surface. Our theoretical calculations do, however, find some surface states in the same region of the SBZ, but about 0.25 eV lower in energy. Occupied electronic surface states have also been determined for the J-K/2-J'/2 symmetry directions of the SBZ. In addition, we have determined several unoccupied surface states along the  $\Gamma$ -J-K/2-J'/2- $\Gamma$  symmetry directions of the  $2 \times 2$  SBZ. As yet, however, there is no experimental data with which to compare these theoretical predictions. Comparison of the electronic structure presented in Fig. 3 with that calculated by Ko *et al.*<sup>19</sup> shows that while the overall topology of the surface state bands obtained by these authors is very similar to that displayed in Fig. 3, the energy separation of these surface bands differs significantly from our calculated values. Experimental studies are also required to discriminate between these different theoretical predictions.

In order to further clarify the effect of the interaction between the Li adatoms and the Si substrate on the electronic

structure, we have also calculated the 3D charge/probability density distributions for all the bands that we have identified as electronic surface states. In total, seven occupied surface state bands, and four unoccupied surface state bands, have been determined in the vicinity of the Fermi energy, as shown in Fig. 3(b).

The low lying occupied electronic surface states denoted by the crosses and the filled squares in Fig. 3(b) represent the silicon dimer  $\sigma$  bonds associated with just the symmetric dimer, and both the symmetric and asymmetric dimers, respectively. Three dimensional charge density plots for the first of these occupied surface state bands are presented in Fig. 4(a) for the  $\bar{K}/2$  symmetry point of the SBZ, together with the corresponding  $\rho_{nk}(z)$  function. Figure 4(b) presents corresponding results for the occupied surface state denoted by the filled squares in Fig. 3(b) for a wave vector between the J'/2 and  $\Gamma$  symmetry points. The occupied electronic surface states denoted by the empty triangles and the filled arrowheads in Fig. 3(b) represent a mixture of the first and third silicon backbond surface states, and the first silicon backbond surface states, respectively. 3D charge density plots for these bands are presented in Fig. 4(c) for the J point of the SBZ (empty triangles), and Fig. 4(d) for a wave vector along the  $\Gamma$ -J symmetry direction (filled arrowheads). All these states are also present on the Si(001)2  $\times$  1-Li surface at 1.0 ML coverage and are not significantly affected by the Li adatoms.<sup>18</sup>

The occupied electronic surface states denoted by the empty squares, empty diamonds and asterisks in Fig. 3(b) represent the silicon dangling bond surface states of the Si symmetric and asymmetric dimers in each  $2 \times 2$  SUC. Plots of the charge density, and the corresponding  $\rho_{nk}(z)$  function, for the surface state denoted in Fig. 3(b) by the empty squares at the J'/2 point of the SBZ, are shown in Fig. 5(a). These plots show significant contributions from the occupied dangling bond orbitals on the up Si atoms of the asymmetric dimers, together with some very small contributions from the occupied dangling bond orbitals localized on the Si atoms of the symmetric dimers. These states can thus be regarded as  $\pi$  orbitals formed on the buckled up Si dimer atoms of the asymmetric dimer. The relatively small dispersion of this surface state band along the  $\Gamma$ -J'/2 symmetry direction (along the dimer row) suggests that any interactions between dimers along a dimer row are relatively weak. It is worth noting that the above description is different to that of Ko *et al.*<sup>19</sup> who identified the corresponding surface state band ( $S_1$ ) of their  $E_1$ - $E_2$  minimum energy configuration as a  $\pi$  band associated with the symmetric (rather than asymmetric) dimers.

3D charge density plots, and the corresponding  $\rho_{nk}(z)$ , calculated at the J'/2 point of the SBZ for the surface states denoted in Fig. 3(b) by the empty diamonds are shown in Fig. 5(b). These plots show significant contributions from both the occupied dangling bond orbitals on the up Si atoms of the asymmetric dimers and the occupied dangling bond orbitals localized on the Si atoms of the symmetric dimers. The relatively small dispersion of this surface state band along the  $\Gamma$ -J symmetry direction (perpendicular to the dimer rows), but quite significant dispersion along the  $\Gamma$ -J'/2 symmetry direction (parallel to the dimer rows), suggests very

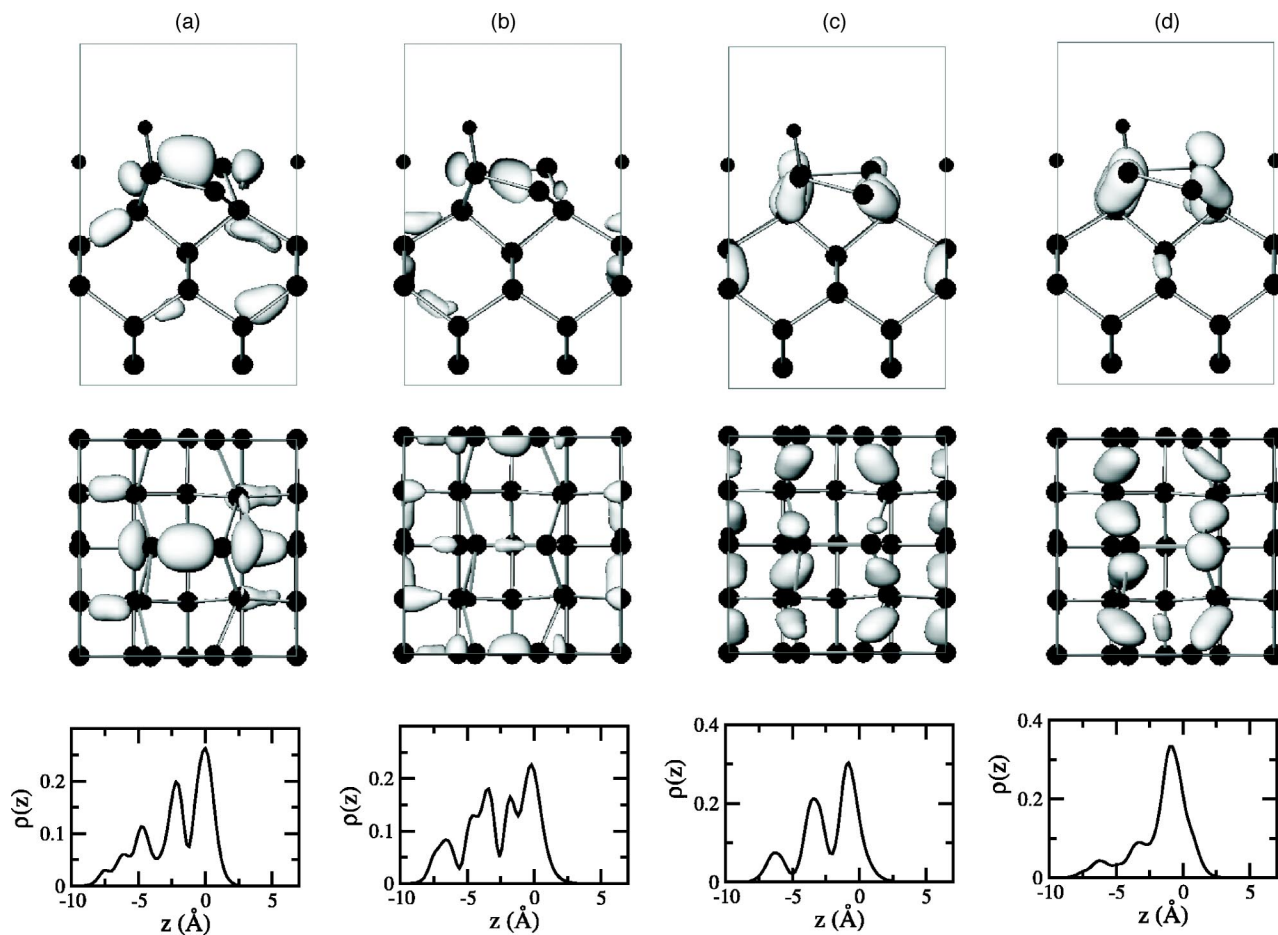


FIG. 4. Side and top views of the 3D charge density distributions, and the corresponding  $\rho_{n\mathbf{k}}(z)$ , for the valence band surface states of the Si(001) $2 \times 2$ -Li chemisorption system at 0.5 ML coverage indicated in Fig. 3(b) by (a) crosses at the K/2 symmetry point of the SBZ, (b) filled squares at a wave vector along the  $J'/2$ - $\Gamma$  symmetry direction of the SBZ, (c) empty triangles at the J point of the SBZ, and (d) filled arrow heads at a wave vector along the  $\Gamma$ -J symmetry direction of the SBZ. The plots are for a charge density isosurface value of  $1.5 \times 10^{-2} e/\text{\AA}^3$ .

weak interaction between the dimer rows but fairly strong interaction between the dimers within a dimer row. This behavior is very similar to the interaction between the dimers on the clean Si(001) $2 \times 1$  reconstructed surface. In contrast to our results, Ko *et al.*<sup>19</sup> claimed that the corresponding surface state band for their adatom topology, which they labelled  $S_2$ , was the  $\pi$  band associated with the asymmetric dimers.

Charge density and  $\rho_{n\mathbf{k}}(z)$  plots for the high-lying surface states denoted by the asterisks in Fig. 3(b), are shown in Fig. 5(c). These plots are for the  $J'/2$  symmetry point of the SBZ. It is clear from these charge density plots that these states have virtually no contribution from the asymmetric dimers and can be regarded as  $\pi^*$  orbitals associated with the symmetric Si dimers. On the Si(001) clean surface with either symmetric or asymmetric dimers, the  $\pi^*$  orbitals are usually unoccupied. For the Si(001) $2 \times 2$ -Li system at 0.5 ML coverage, however, the energies of these orbitals are pushed below the Fermi level by the charge transfer of  $\sim 2e$  from the two Li adatoms to the Si dimer. As a result, these symmetric dimer  $\pi^*$  orbitals become occupied.

The lowest energy unoccupied surface state band denoted by the empty circles in Fig. 3(b) represents the empty dan-

gling bond orbitals associated with the down Si atoms of the asymmetric dimers of the Si(001) $2 \times 2$ -Li chemisorbed surface. This is clearly seen from the 3D probability density plots shown in Fig. 6(a). These surface states, which are clearly the  $\pi^*$  antibonding states associated with the asymmetric dimers, are analogous to the lowest unoccupied energy band eigenstates of the clean Si(001) $2 \times 1$  surface.<sup>25</sup> These results show that the  $\pi^*$  surface state associated with the asymmetric dimers (LUMO) lies well above the  $\pi^*$  surface state associated with the symmetric dimers (HOMO). The resulting bandstructure of the Si(001) $2 \times 2$ -Li chemisorption system at 0.5 ML is thus predicted to be semiconducting in agreement with experiment. This is a direct result of the charge from the lithium adatoms being transferred to the down Si atom of just one of the dimers in each  $2 \times 2$  SUC (see Fig. 2).

Three-dimensional probability density plots for the unoccupied electronic surface state bands denoted by the empty inverted triangles, the filled circles and the filled triangles in Fig. 3(b) are presented in Figs. 6(b), 6(c), and 6(d), respectively. These correspond to wave vectors at the K/2 point, the J point, and along the J-K/2 symmetry direction of the SBZ. It is clear from Fig. 6(b) that the surface states repre-



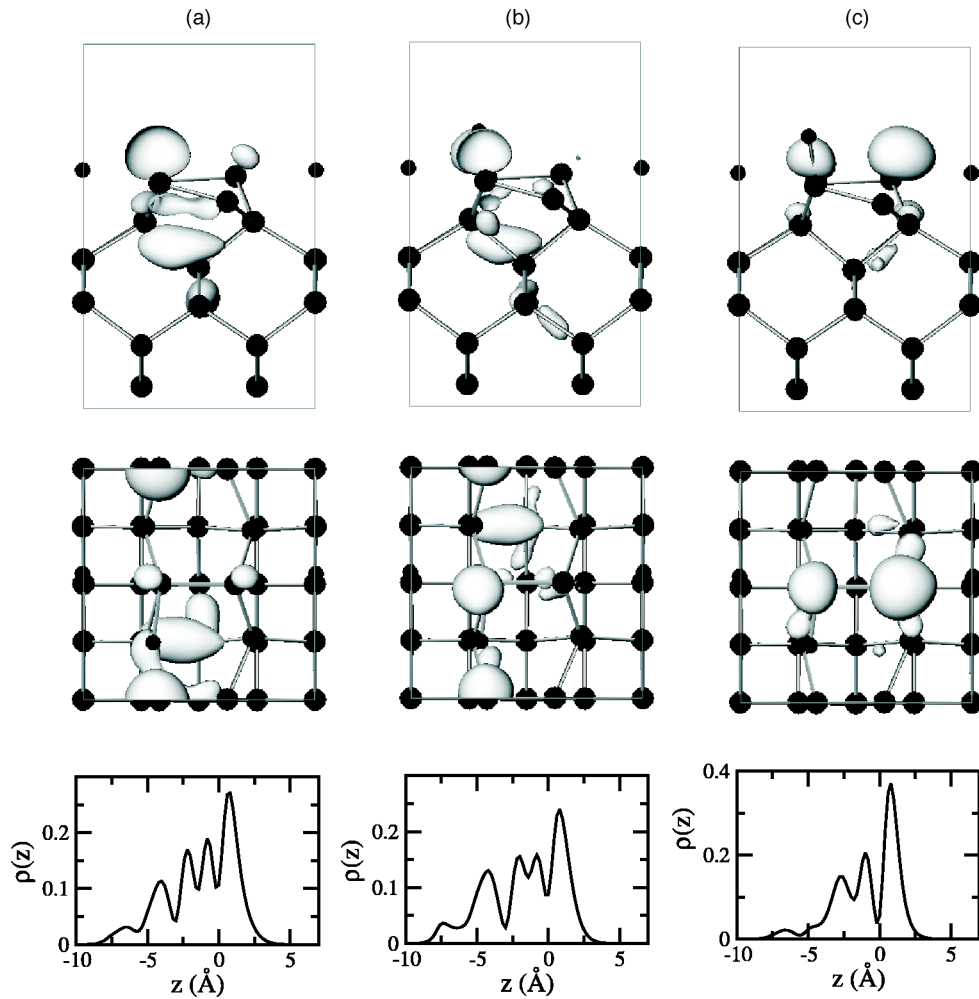


FIG. 5. Side and top views of the 3D charge density distributions, and the corresponding  $\rho_{nk}(z)$ , for the surface states of the Si(001) $2 \times 2$ -Li chemisorption system at 0.5 ML coverage indicated in Fig. 3(b) by (a) empty squares, (b) empty diamonds, and (c) asterisks. All of these plots are for a wave vector at the  $J'/2$  symmetry point of the SBZ. The first two charge density plots are for an isosurface value of  $1.5 \times 10^{-2} e/\text{\AA}^3$ , while the third set corresponds to  $2.0 \times 10^{-2} e/\text{\AA}^3$ .

sented by the empty inverted triangles in Fig. 3(b) correspond to a combination of the  $\sigma^*$  antibonding orbitals of the symmetric dimers and orbitals from the lower Li adatoms at the D sites. The surface states denoted by the filled circles in Fig. 3(b) also involve the  $\sigma^*$  antibonding orbitals of the symmetric dimers, but now the coupling is to orbitals from the upper Li adatoms at the E sites. This is evidenced by the significant rotation and distortion of the symmetric dimer  $\sigma^*$  orbitals produced by the upper lithium atoms [see Fig. 6(c)]. The unoccupied surface state band denoted by the filled triangles in Fig. 3(b), on the other hand, is made up almost exclusively of  $\sigma^*$  antibonding orbitals associated with the asymmetric Si dimers [see Fig. 6(d)]. It is worth noting that only the first of these surface states contains a significant contribution from the lower Li adatoms. It follows that this unoccupied surface state may play an important role in discriminating between our minimum energy structures, in which the lower lithium atom occupies a  $D_1$  or  $D'_1$  site, and those of Morikawa *et al.*<sup>17</sup> and Ko *et al.*<sup>19</sup> where both lithium atoms occupy E sites.

#### IV. SUMMARY

The plane wave pseudopotential DFT method contained in the VASP code has been used to investigate the atomic and electronic structure of the Si(001) $2 \times 2$ -Li chemisorption system at 0.5 ML coverage. Two essentially degenerate Li adatom configurations involving almost identical reconstruction of the substrate into a mixture of alternating symmetric and asymmetric Si-Si dimers were found to be the most stable. The calculations have shown that the transfer of charge from the lithium adatoms to just one of the dimers in each  $2 \times 2$  SUC causes those dimers to become approximately symmetric, while leaving the other antibuckled dimers essentially unchanged. Our calculated electronic structure supports the model of two topologically different subsystems for the Li chemisorbed Si(001) $2 \times 2$  substrate at 0.5 ML coverage. It also provides strong evidence for substantial charge transfer from the Li adatoms to the substrate, and strong polar bonding between the lithium atoms and the Si(001) $2 \times 2$  surface. It is the combination of these

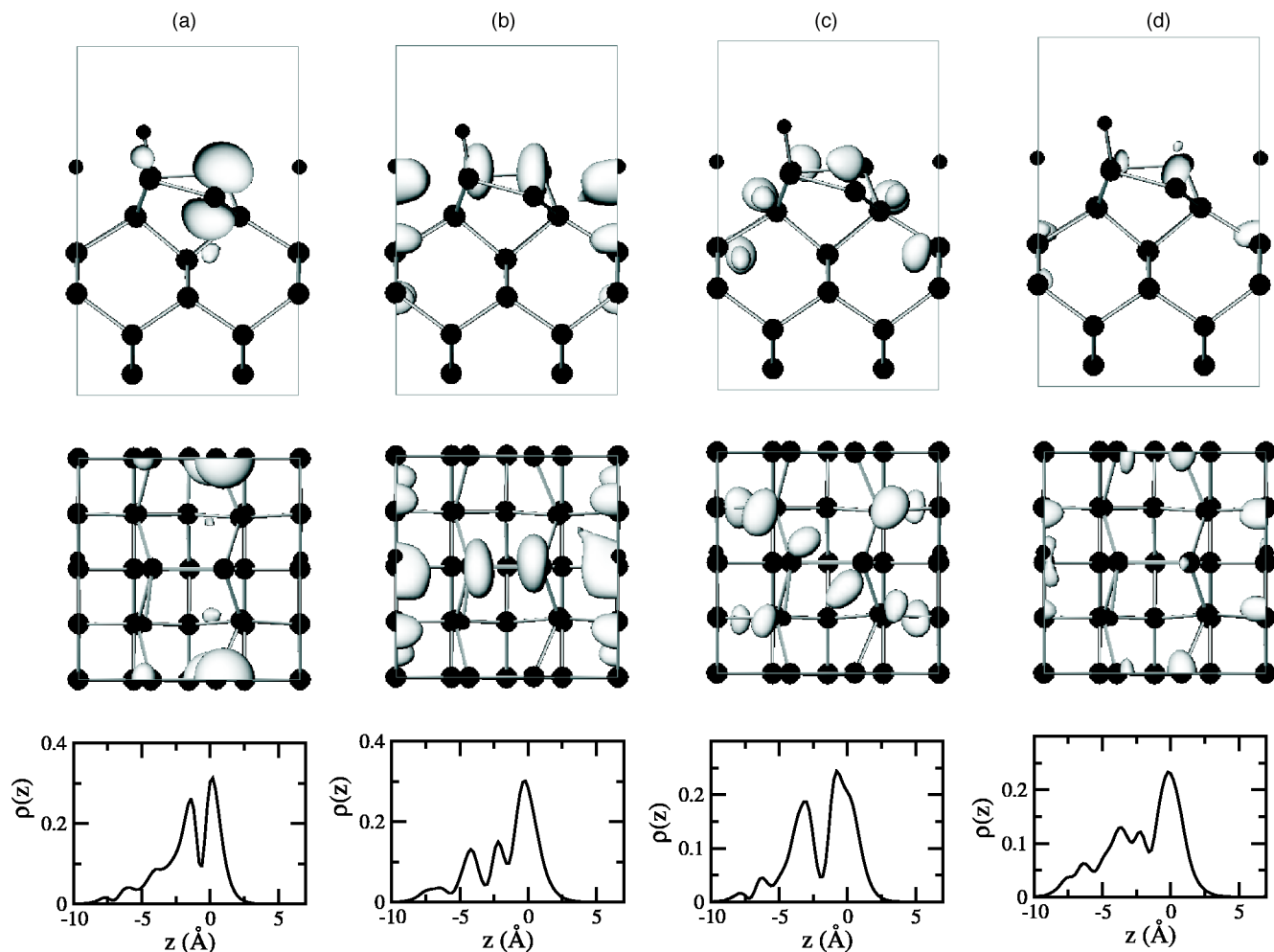


FIG. 6. Side and top views of the 3D probability density distributions, and the corresponding  $\rho_{nk}(z)$ , for the surface states of the Si(001) $2 \times 2$ -Li chemisorption system at 0.5 ML coverage indicated in Fig. 3(b) by (a) empty circles at the  $J'/2$  symmetry point of the SBZ, (b) empty inverted triangles at the  $K/2$  symmetry point of the SBZ, (c) filled circles at the  $J$  point of the SBZ, and (d) filled triangles at a wave vector along the  $J$ - $K/2$  symmetry direction of SBZ. The plots in (a) are for a probability density isosurface value of  $2.0 \times 10^{-2} \text{ \AA}^{-3}$ , while those in (b)–(d) are for the value  $1.5 \times 10^{-2} \text{ \AA}^{-3}$ .

effects that explains the nonmetallic behavior of the Si(001) $2 \times 2$ -Li system at low coverage, as confirmed experimentally by Johansson and Reihl.<sup>5</sup>

We have identified both occupied and unoccupied surface states in the vicinity of the Fermi energy, and investigated the detailed nature of these states. The predicted occupied surface state bands were found to be in good agreement with the current ARUPS data. The electronic structure of the Li/Si(001) $2 \times 2$  system is unique in that it also contains a number of occupied surface state bands that originate exclusively from the asymmetric dimers and are not affected by the chemisorption of the Li atoms. The lowest energy unoccupied surface state band has been shown to correspond to the  $\pi^*$  antibonding state of the asymmetric dimers. We

would thus expect the Si(001) $2 \times 2$ -Li chemisorption system at 0.5 ML coverage to exhibit similar reactivity to that of the clean Si(001) surface. The second and third lowest unoccupied surface states were found to involve significant contributions from the Li adatoms, and the resulting surface state bands exhibited a clear dependence on the actual Li adatom configuration.

#### ACKNOWLEDGMENTS

One of us (H.Q.S) would like to thank the Australian Government and the University of Newcastle for financial support. We would also like to acknowledge the APAC Supercomputing Facility for the provision of computing resources.



- <sup>1</sup>See articles in *Physics and Chemistry of Alkali Metal Adsorption*, edited by H. P. Bonzel, A. M. Bradshaw, and G. Ertl (Elsevier, Amsterdam, 1989).
- <sup>2</sup>*Metallization and Metal-Semiconductor Interfaces*, NATO Advanced Study Institutes, Ser. B, edited by I. P. Batra (Plenum, New York, 1989), Vol. 195.
- <sup>3</sup>R. I. G. Uhrberg and G. V. Hansson, *CRC Crit. Rev. Solid State Mater. Sci.* **17**, 133 (1991).
- <sup>4</sup>H. Tochiyama and Y. Murata, *Surf. Sci.* **215**, L323 (1989).
- <sup>5</sup>L. S. O. Johansson and B. Reihl, *Surf. Sci.* **287/288**, 524 (1993).
- <sup>6</sup>M. Eckhardt, H. Kleine, and D. Fick, *Surf. Sci.* **319**, 219 (1994).
- <sup>7</sup>H. Kleine, M. Eckhardt, H. J. Jänsch, and D. Fick, *Surf. Sci.* **323**, 51 (1995).
- <sup>8</sup>C. Y. Kim, K. S. Shin, K. D. Lee, and J. W. Chung, *Surf. Sci.* **324**, 8 (1995).
- <sup>9</sup>L. S. O. Johansson, T. M. Grehk, S. M. Gray, M. Johansson, and A. S. Flodström, *Nucl. Instrum. Methods Phys. Res. B* **97**, 364 (1995).
- <sup>10</sup>T. M. Grehk, L. S. O. Johansson, S. M. Gray, M. Johansson, and A. S. Flodström, *Phys. Rev. B* **52**, 16 593 (1995).
- <sup>11</sup>M. K.-J. Johansson, S. M. Gray, and L. S. O. Johansson, *Phys. Rev. B* **53**, 1362 (1996).
- <sup>12</sup>K. D. Lee, C. Y. Kim, and J. W. Chung, *Surf. Sci.* **366**, L709 (1996).
- <sup>13</sup>C. Y. Kim, H. W. Kim, J. W. Chung, K. S. An, C. Y. Park, A. Kimura, and A. Kakizaki, *Appl. Phys. A: Mater. Sci. Process.* **64**, 597 (1997).
- <sup>14</sup>S. Hongo, S. Kaneko, and T. Urano, *Surf. Sci.* **433-435**, 775 (1999).
- <sup>15</sup>K. Kobayashi, S. Blügel, H. Ishida, and K. Terakura, *Surf. Sci.* **242**, 349 (1991).
- <sup>16</sup>P.-L. Cao, R.-H. Zhou, and X.-Y. Zhou, *Phys. Lett. A* **159**, 179 (1991).
- <sup>17</sup>Y. Morikawa, K. Kobayashi, and K. Terakura, *Surf. Sci.* **283**, 377 (1993).
- <sup>18</sup>H. Q. Shi, M. W. Radny, and P. V. Smith (submitted for publication).
- <sup>19</sup>Y.-J. Ko, K. J. Chang, and J.-Y. Yi, *Phys. Rev. B* **56**, 9575 (1997).
- <sup>20</sup>J. D. Levine, *Surf. Sci.* **34**, 90 (1973).
- <sup>21</sup>G. Kresse and J. Hafner, *Phys. Rev. B* **47**, 558 (1993); G. Kresse and J. Hafner, *ibid.* **49**, 14 251 (1994).
- <sup>22</sup>G. Kresse and J. Furthmüller, *Comput. Mater. Sci.* **6**, 15 (1996).
- <sup>23</sup>G. Kresse and J. Furthmüller, *Phys. Rev. B* **54**, 11169 (1996).
- <sup>24</sup>G. Kresse and D. Joubert, *Phys. Rev. B* **59**, 1758 (1999).
- <sup>25</sup>A. Ramstad, G. Brocks, and P. J. Kelly, *Phys. Rev. B* **51**, 14 504 (1995).